THE JOURNAL OF PHYSICAL CHEMISTRY B

Article

Quantifying Changes in the High-Frequency Dynamics of Mixtures by Dielectric Spectroscopy

Tatiana Psurek, Christopher L. Soles, Kirt A. Page, Marcus T. Cicerone, and Jack F. Douglas

J. Phys. Chem. B, **2008**, 112 (50), 15980-15990 • Publication Date (Web): 26 September 2008

Quantifying Changes in the High-Frequency Dynamics of Mixtures by Dielectric Spectroscopy†

Tatiana Psurek,* Christopher L. Soles, Kirt A. Page, Marcus T. Cicerone, and Jack F. Douglas*

Polymers Division, National Institute of Standards and Technology, Gaithersburg, MD 20899

Received: April 20, 2008; Revised Manuscript Received: August 5, 2008

Additives to polymeric materials can lead to appreciable changes in the rates of relaxation and reaction in these mixtures that can profoundly alter material properties and function. We develop a general theoretical framework for quantifying changes in the "high-frequency" relaxation dynamics of mixtures based on classical transition state theory, in conjunction with mathematical statements regarding the dependence of the entropy (S^+) and enthalpy (E^+) of activation of the high-frequency relaxation time on diluent mass fraction, x_w. Specifically, we deduce a general classification scheme for diluents based on a consideration of the sign of the differential change in S^+ and E^+ with x_w. Two of these classes of diluents exhibit a transition from plasticization to antiplasticization (defined specifically as a speeding up or slowing down of relaxation relative to the pure system, respectively) upon varying temperature through an "antiplasticization" temperature, T_{anti}. Extensive dielectric relaxation measurements on polycarbonate (PC) as a function of temperature and diluent (Aroclor) concentration are utilized to illustrate our theoretical model, and we focus particularly on the Arrhenius "β" dielectric relaxation process of these mixtures. Many aspects of our scheme for quantifying changes in the high-frequency dynamics of mixtures are rationalized by our mixture model. In particular, we show that the dilution of PC by Aroclor is consistent with a theoretically predicted (one of the two antiplasticization mixture classes mentioned above) transition from antiplasticization to plasticization with decreasing temperature. We briefly compare our findings from dielectric measurements with those from elastic incoherent neutron scattering and dynamical−mechanical measurements, providing further evidence for the antiplasticization-to-plasticization transition phenomena that we observe in our high-frequency dielectric measurements.

I. Introduction

The introduction of solvents and nanoparticle additives to biological and synthetic polymeric materials can have a tremendous impact on the processing characteristics, functioning, and stability of diverse materials. Currently, the investigation of this phenomenon is particularly active in connection with the preservation and modification of the aesthetic properties of foods, the preservation of tissues and drugs, and with studies aimed at understanding toxicity effects arising from environmental exposure to additives that disrupt natural biological function. In synthetic polymers, there is active research relating to the enhancement of the mechanical stability of polymer films, the control of the gas permeability of polymeric films and bulk materials, as well as in the development novel nanocomposite materials. Given this diverse activity, there is evidently a need for a theoretical framework for understanding and controlling basic property changes in these complex mixtures (e.g., tensile strength, stiffness, heat distortion, elongation, impact strength, gas permeability, reaction rates, etc.).

In the present work, we investigate this general problem using the synthetic polymer polycarbonate (PC) and the diluent Aroclor 1260 (a commercial name for polychlorinated biphenyl mixture with 60% chlorine); this is a classical model system in which large dilution-induced changes in mechanical properties have been well documented.[1] Such synthetic model mixtures are advantageous in initial studies aimed at developing a framework for these property changes since the molecular structure (mass, side groups) can be tuned with considerable control,[2] allowing us to explore how molecular properties influence dynamical−mechanical properties. We choose dielectric spectroscopy as our primary experimental methodology because it is readily available in many academic and commercial laboratories and because this methodology can access the relatively high-frequency regime describing the *local* segmental dynamics of the polymer.

Although our experimental focus is on the relatively high-frequency "β" or "secondary" dielectric relaxation process of PC, we are concerned with using this data in developing a *general method* for quantifying how molecular additives influence alter high-frequency relaxation processes in liquids. We restrict our attention to relaxation process that do not involve highly cooperative or intermittent molecular motions, and which correspondingly exhibit relaxation times having a nearly Arrhenius temperature dependence. This choice is not overly restrictive since most high-frequency relaxation processes in condensed materials appear to satisfy this relationship over a wide temperature range. We develop a framework for describing changes in the high-frequency dynamics of mixtures based on a simple transition state theory framework, which is consistent with Arrhenius temperature-dependent relaxation times.[3,4]

Our previous study of high-frequency dielectric relaxation in mixtures of trehalose and glycerol[4,5] was aimed at understanding antiplasticization in model trehalose−glycerol mixtures as a process relevant to protein preservation and, in this specific context, we defined the ratio θ of the high-frequency relaxation

† Part of the "Karl Freed Festschrift".

* To whom correspondence should be addressed. E-mail: tp@usp.org (T.P.); jack.douglas@nist.gov (J.F.D.).

10.1021/jp8034314 CCC: $40.75
Published on Web 09/26/2008

time for the mixture $\tau_{(mixture)}$ to the one of "pure" species $\tau_{(pure)}$ as a basic quantity for investigation,[5]

$$\theta = \tau_{(mixture)}/\tau_{(pure)} \quad (1)$$

The slowing down of the high-frequency dynamics by an additive is a defining characteristic of "antiplasticization",[5] while speeding up of the dynamics characterizes "plasticization".[5] (Notably, this phenomenon is *not* generally correlated to changes in the low frequency fluid dynamics such as the zero shear viscosity and the glass transition temperature, although the addition of additives changes this aspect of the fluid dynamics, as we shall discuss below.) Thus, we refer to a mixture as "plasticized" if the "antiplasticization parameter" obeys the relation $\theta < 1$ and "antiplasticized" for $\theta > 1$. The temperature where $\theta = 1$ defines the "antiplasticization temperature", T_{anti} where the additive makes *no change* in the fluid relaxation time. Evidently, T_{anti} is some kind of compensation temperature where the mixture is "ideal" in some sense and we show how this quantity can be estimated in our modeling section. In most polymer fluids (at least to the extent such things have been investigated[5]), antiplasticization is found well below the glass transition temperature, T_g. This is a "normal" trend in cases where antiplastization is observed.[5,6]

Our previous investigation of treahalose−glycerol[5] mixtures confirmed this expected trend, indicating antiplasticization in the low temperature glass state based on high-frequency ("β") dielectric relaxation measurements and plasticization at more elevated temperatures (below T_g). This result was also confirmed qualitatively by independent incoherent neutron scattering and spectroscopy measurements (see ref 5 for discussion), and recently this effect has also been confirmed by atomistic molecular dynamics simulations.[7,8] The novelty of our previous work[5] is the high level of quantification of the change in the high-frequency dynamics that was achieved by dielectric spectroscopy, the precise identification of the temperature where the change plasticization to antiplasticization occurs upon cooling, and the theoretical framework developed to explain these changes in the high-frequency mixture relaxation time of trehalose as a function of diluent (glycerol) concentration and temperature. Extending these measurements and the corresponding theoretical framework[5] to PC/Aroclor mixtures led us (fortuitously) to the first quantitative observation of the *opposite situation*: plasticization in the low temperature glass regime and antiplasticization at higher temperatures. These observations obviously provide a challenge for theoretical explanation, and we show below that a generalization of our former theoretical treatment[5] naturally explains these opposing antiplasticizing trends with temperature.

Of course, not all high-frequency relaxation processes, involving relatively local molecular motions, compared to those involved in structural (α) relaxation, will be shifted in the same way by additives, and only some of these relaxation processes can be expected to be of direct relevance in connection with observable mechanical properties and the physics of glass-formation. This situation requires the comparison of the selected high-frequency relaxation process, and its changes with dilution, with independent mechanical measurements and other high-frequency measurements that provide insight into the stiffness of the material to establish the predictive significance of observed changes in the "high-frequency" dielectric measurements. Accordingly, we briefly compare our dielectric measurements with incoherent neutron scattering and mechanical relaxation measurements to characterize and compare how the antiplastization effect is exhibited in these measurements.

Of course, some differences (e.g., the precise value of the antiplasticization temperature) are expected because of the very different frequency ranges explored in these relatively "high-frequency" measurements. Thus, while all our measurements below exhibit a common trend in the transition between plasticization and antiplasticization as the temperature is varied, there are quantitative differences in the exact compensation or antiplasticization temperature, etc. (Evidently, there is some uncertainty in the specification of the antiplasticization temperature, but there is no uncertainty in the determination of T_{anti} of a particular relaxation process.)

The complementary neutron and viscolelastic measurements further remind us that the term "high-frequency" relaxation is *relative*, and it is always possible to define even higher frequency relaxation processes in condensed phases of matter. Our dielectric measurements specifically focus on the Johari−Goldstein (JG) or "β-relaxation" process that is conspicuously and generally observed in glass-forming liquids in dielectric and calorimetric measurements in a frequency range higher than the α-relaxation process and for a temperature range where those relaxation processes can be resolved from each other.[9,10] Very high-frequency ("fast") relaxation processes (typically in the range of 10^{-12} s to 10^{-9} s) are often studied in glass-forming liquids in connection with small-scale density fluctuations in dynamic neutron scattering measurements, and computational limitations often limit molecular dynamics simulations to this time regime. Importantly, the JG (β-relaxation) process has been shown to be *directly linked* in phenomenology to the α-relaxation process.[10] Although there is no general agreement on the exact nature of the local molecular motions responsible for the dielectric β-relaxation process, this "secondary" relaxation process is commonly interpreted in terms of the elementary local collective motions from which the larger scale collective motions associated with the α-relaxation process are comprised.[10] The dielectric β-relaxation process is thus an obvious candidate for quantifying the freezing of the high-frequency dynamics of fluids.

II. Materials and Measurements

A. Materials. Poly(Bisphenol A carbonate) (PC) with an average molecular mass of 64 000 g/mol was purchased from Aldrich Chemicals Co. and dissolved in dichloromethane (DCM) to obtain a 10% solution by relative polymer mass. Then, Aroclor 1260 was added to the solutions at mass fractions x_w of 0.05, 0.1, 0.15, 0.2, relative to the PC. These solutions were left to evaporate the DCM in air at room temperature for 12 h. The samples were then kept under vacuum at $T = 505$ K for another 12 h to ensure solvent removal. After this time, the samples were formed by melt pressing at $T = 473$ K for a few minutes. This strategy resulted in samples having a thickness of about 0.07 mm to 0.09 mm.

B. Differential Scanning Calorimetry (DSC). DSC measurements were preformed on the TA Instruments DSC Q1000 analyzer. All samples were analyzed in the temperature range from 303 to 523 K with the heating/cooling rate of 10 K/min. An appreciable step, indicating the glass transition temperature, T_g, has been observed for all the samples. The standard uncertainty of the method was about 5%.

C. Dielectric Spectroscopy. The film samples were placed between parallel gold-plated flat electrodes (Novocontrol) and measured in a frequency range between 0.1 Hz and 1 MHz using an Alpha-A High Performance Frequency Analyzer from Novocontrol Technologies. The measurements have been performed in a temperature range between 153 and 483 K. All the

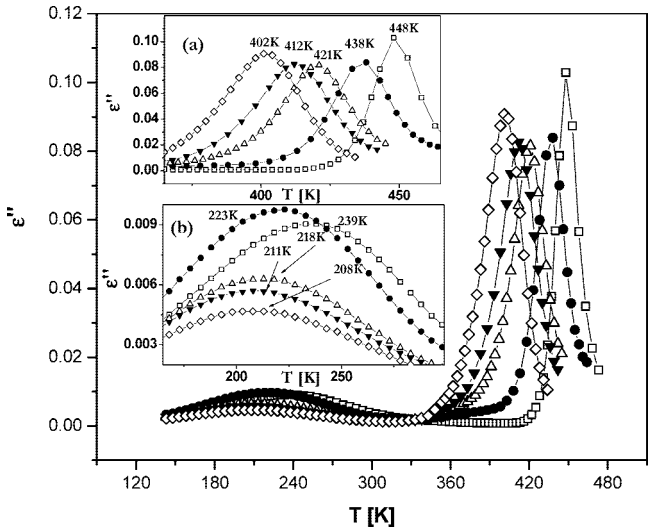

Figure 1. Dielectric loss, at 60 kHz, as a function of temperature for mixtures with Aroclor mass fraction, x_w: 0-squares; 0.05-circles; 0.1-up triangles; 0.15-down triangles; 0.2-diamonds. The insets present magnified curves in the region of α-relaxation (a) and β-relaxation (b), and the values given are temperatures where peaks have their maxima.

experiments have been performed under isothermal conditions, and the standard uncertainty of the method was about 10%.

D. Neutron Scattering. The incoherent neutron scattering experiments were performed at the NIST Center for Neutron Research on the high flux backscattering spectrometer (HFBS), located on the NG2 beamline. The standard uncertainty of the method was in order of 1%. This spectrometer utilizes cold neutrons with a wavelength of 6.271 Å and probes motions over a reciprocal space range of 0.25 $Å^{-1} < Q < 1.75$ $Å^{-1}$. The 0.8 μeV full width at half-maximum energy resolution of this spectrometer means motions slower than 200 MHz appear as static and contribute to the elastic scattering. The HFBS spectrometer was operated in the "fixed window mode", where the sample was ramped at 1 K/min from approximately 50 K to a final temperature that was well above the T_g of the PC/Aroclor mixtures. The decrease in the intensity of the elastic scattering peak was recorded as a function of T and Q. For elastic incoherent scattering, the Q dependence of this elastic scattering is often approximated with the Debye−Waller factor:

$$I_{\text{inc,elastic}}(Q) \propto \exp\left(-\frac{1}{3}Q^2\langle u^2\rangle\right) \tag{2}$$

Within this model, based on a harmonic oscillator, the slope of $\ln(I_{\text{inc,elastic}}(Q))$ versus Q^2 is equal to $\langle u^2\rangle/3$. While most atomic motions in soft condensed matter are admittedly anharmonic, this approximation has been found to be practically useful in characterizing the dynamics in both synthetic[11−15] and biological[16−20] macromolecules.

E. Dynamical Mechanical Analysis (DMA). DMA of the films was performed on a TA Instruments DMA Q800 analyzer in tensile mode using clamps for thin film samples. The standard uncertainty of the method was about 10%. All samples were analyzed at a frequency of 1 Hz over a temperatures range from 133 to 470 K with a heating rate of 2 K/min.

III. Results

Figure 1 illustrates the imaginary part of permittivity ε'', as a function of temperature, in the frequency of 60 kHz, for pure PC (squares) and its mixtures with Aroclor with the weight fractions $x_w = 0.05$ (circles), 0.1 (upward pointing triangles), 0.15 (downward pointing triangles), and 0.2 (diamonds). Two relaxation peaks are observed. A prevalent α-relaxation process at higher temperatures and a β-relaxation process at lower temperatures are apparent, and the insets provide enlargements of these peaks. Qualitatively, we see a progressive shift in Figure 1 of both relaxation processes to lower temperatures with dilution, consistent with *plasticization* in the low temperature glass state, and we quantify this trend below.

We contrast our observations with previous ones on the addition of tris(2-ethyl)phosphate (TOP) to PC over a similar temperature range. In this system, the β-relaxation peak, observed by DMA, shifts to higher temperatures, while T_g decreases.[21,22] This corresponds to classic *antiplasticization* (slowing down of the high-frequency relaxation despite the reduction of the glass transition temperature) in the glassy state. Plasticization of the high-frequency dynamics has also been qualitatively observed both by dielectric spectroscopy and DMA in nearly the same temperature range with the addition of TOP to tetramethylbisphenol A polycarbonate (TMBPA-PC),[23] in accord with our observations. Previous work has established trends in the observation of plasticization or antiplasticization in the low temperature glass state with variation in the additive structure and interaction.[20] The physics of this counterintuitive change in fluid dynamics has been explored recently in molecular dynamics simulation,[24−27] where the effect is attributed to the consequences of the modification of fluid molecular packing by the additive.

A firm assignment of a transition from plasticization to antiplasticization with temperature can not be determined from Figure 1, since this relaxation process (i.e., peak in dielectric spectra as a function of temperature at fixed frequency) is only observed in the low temperature glass state.

A. High-Temperature Relaxation. Although our main purpose in the present work is to characterize the change in the high-frequency dynamics of the reference system (PC) through the addition of diluent (Aroclor), it is important to characterize how the long-time α-relaxation associated with cooperative molecular motions and the glass-formation become modified by the diluent. Of course, the effects of diluents on the α-relaxation dynamics in polymers have been exhaustively studied in previous work so we concentrate only on some of the essential aspects of these changes relevant to the current study. In particular, we examine how the diluent modifies the temperature dependence of the α-relaxation time, τ_α, and thus the fragility of glass-formation, and we also determine the variation of the glass transition temperature T_g with the concentration of Aroclor based on DSC.

The results obtained from dielectric measurements, for each relaxation process, have been analyzed in term of Havriliak−Negami (HN) relationship (eq 3),[28] which applies to high-frequency condensed matter relaxation processes with remarkable universality.[29,30] The general HN relaxation function,[28]

$$\varepsilon^* = \varepsilon_\infty + \frac{\Delta\varepsilon}{\left[1 + (j\omega\tau_{\text{HN}})^\alpha\right]^\beta} \tag{3}$$

is a natural candidate for characterizing dielectric data of glassy materials. In eq 3, $\omega = 2\pi f$, ε^* is the relative complex dielectric permittivity, $\varepsilon^* = \varepsilon' - j\varepsilon''$, ε_∞ denotes the asymptotic value of the permittivity at high frequency, $\Delta\varepsilon$ is the dielectric strength, τ_{HN} is the relaxation time of the dielectric process, and α and β ($0 < \alpha \leq 1$ and $0 < \alpha\,\beta \leq 1$) are the "shape" or fluid "memory" parameters that describe the symmetric and asymmetric broadening of the dielectric function. We note that when

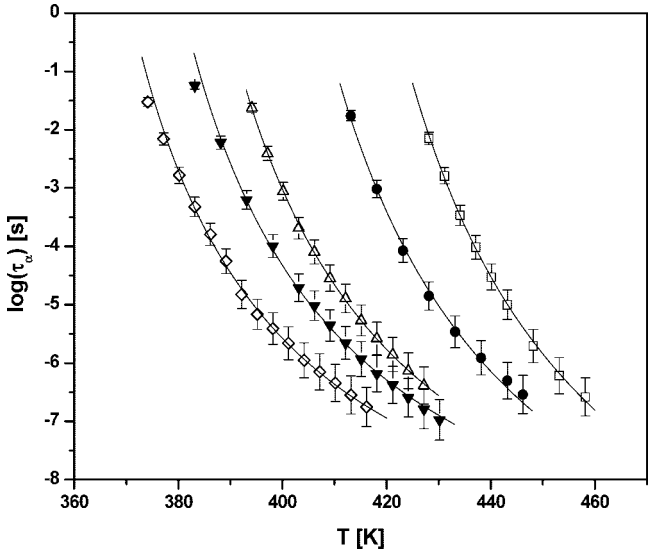

Figure 2. Relaxation time as a function of temperature for α-relaxation process. Lines are fits to the VF equation, points are experimental values (symbols are the same as in Figure 1).

$\beta = 1$, the HN relaxation function becomes the Cole−Cole function,[29−31] which describes materials exhibiting a broad and symmetric distribution of relaxation times. This kind of relaxation process is usually observed for relatively "local" relaxation in macromolecules in comparison to long time α-relaxation, exhibiting a nonsymmetrical and a much narrower peak (see Figure 1 insets). We refer to the relative slow α and fast β relaxation times as τ_α and τ_β, respectively. It has been shown that the relaxation time obtained from fitting to the HN equation depends on the values of parameters α and β.[32] For this reason, another definition of relaxation time: $\tau = 1/(2\pi f_{max})$, where f_{max} indicates the frequency in which ε'' has its maximum, is often used, and this definition is implemented in our study.

It is characteristic feature of high-frequency relaxation processes that the relaxation time has an Arrhenius temperature dependence, and our measurements indeed indicate that our dielectric β-relaxation time τ_β obeys the relationship[3,4]

$$\tau_\beta = \tau_\infty \exp(E^+/RT) \quad (4)$$

where E^+ is the β-relaxation activation energy, R is the gas constant, and τ_∞ is the β-relaxation time prefactor. A characteristic features of τ_∞ from dielectric β-relaxation measurements is that it is commonly observed to correspond to an extremely small time scale in the range (10^{-13} s to 10^{-18} s),[33] and below we consider some arguments that have been made to rationalize this phenomenon.

In contrast to β-relaxation, the long-time segmental structural relaxation time τ_α, associated with the large-scale collective molecular motion that accompanies glass-formation,[34,35] is characteristically non-Arrhenius[7,9] and Figure 2 illustrates estimates of the temperature dependence of τ_α obtained from our dielectric relaxation measurements. The symbols represent data determined by fitting to the HN equation and the lines are fits to the Vogel−Fulcher (VF) relation,[36]

$$\log \tau_\alpha = \log \tau_0 + \frac{D_f T_0}{T - T_0} \quad (5)$$

where the α-relaxation time prefactor τ_0 typically has an order of magnitude $\tau_0 \sim O(10^{-13}$ s), T_0 is the VF temperature where the relaxation time extrapolates to an infinite time, and the dimensionless "fragility parameter" D_f provides a measure of how much the relaxation deviates from an Arrhenius relation. Fluids that exhibit VF temperature of structural relaxation have been termed "fragile" and D_f is accordingly often taken as a quantitative measure of the "fragility" of glass-formation.[17,37] Sometimes the fragility parameter is alternatively defined as $K = 1/D_f$, which increases as the fragility of the glass-formation increases.[15,17,38]

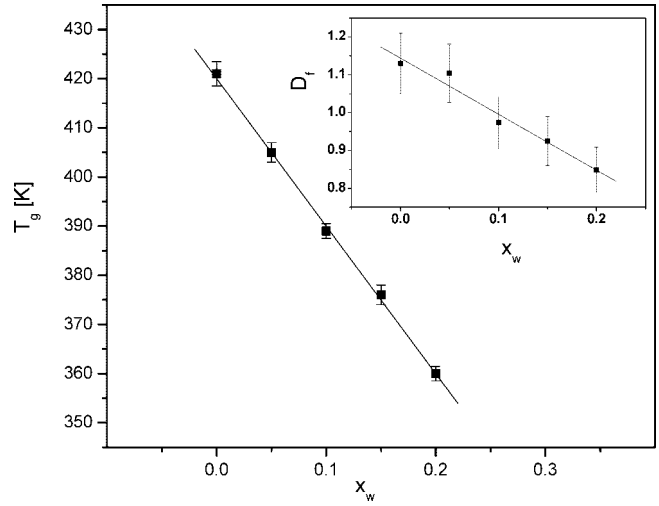

Figure 3. Calorimetric glass transition temperature vs Aroclor mass fraction. The inset presents the VF parameter D_f as a function of Aroclor concentration.

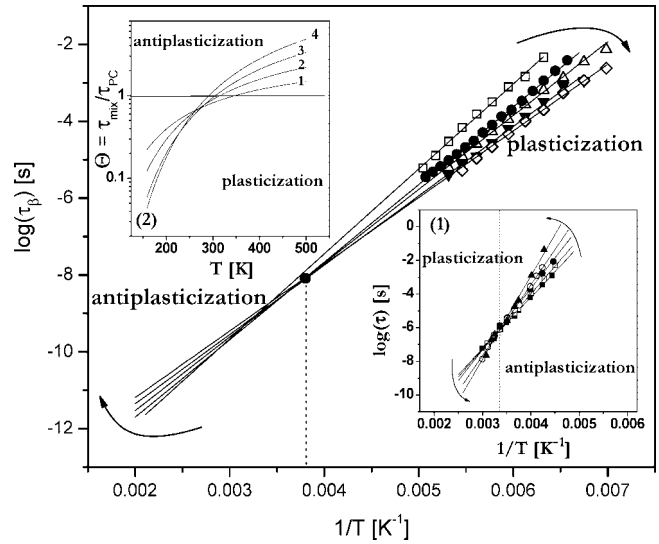

Figure 4. Temperature dependence of β-process relaxation time. Lines are fits to the Arrhenius equation, and the points are experimental data (symbols are the same as in Figure 1). The error of relaxation time values is about 5%. Inset 1 shows relaxation time data obtained for trehalose−glycerol mixtures; $x_{w\_glycerol}$: closed squares-0; open squares-0.05; closed circles-0.1; open circles-0.15; closed triangle-0.2. Inset 2 presents θ for mixtures with Aroclor mass fraction x_w: (1) 0.05, (2) 0.1, (3) 0.15, (4) 0.2. The fitted curves shown in this inset do not intersect at $\theta = 1$ because of the uncertainty in the data fit in the main figure.

The glass transition temperature T_g is another basic characterization parameter of glass-forming liquids, and for completeness we also consider this quantity as a function of dilution, even though our focus in the present paper is on the high-frequency relaxation processes. The DSC estimates of T_g for our mixtures shown in Figure 3 indicate a linear decrease of T_g with an increasing diluent concentration, and the inset presents the corresponding variation of D_f, obtained by fitting the data

in Figure 2 to the VF relation, eq 5. As in the case of T_g, the fragility parameter D_f also progressively decreases with an increasing Aroclor concentration. This means that the fragility of PC of the glass-formation *increases* upon dilution by Aroclor, a situation *opposite* to our previous findings for the addition of glycerol to trehalose.[5] Enhanced fragility upon dilution has also been observed in the addition of trehalose to water[39] and upon the addition of water to glycerol,[40] an effect that has potential ramifications to the preservation of biological materials in aqueous media.

B. Plasticization−Antiplasticization Transition in PC/Aroclor. As mentioned before, the relaxation peaks in dielectric data presented in Figure 1 indicate plasticization in the glass state since both peaks are shifted to lower temperatures. More generally, introducing an additive should shift the β-relaxation peak time to a lower or higher value at a fixed temperature, corresponding to plasticization or antiplasticization, respectively. This definition allows us to consider plasticization versus antiplasticization as a function of temperature. Accordingly, Figure 4 shows the variation of τ_β for PC diluted by Aroclor obtained by fitting our dielectric data to the HN equation. We admit that the PC secondary relaxation peak is somewhat weak and broad and that our frequency range is limited, which restricts the temperature range of our observations to a range of about 50 K. Nevertheless, we find that the Arrhenius curves for τ_β intersect at a common point, allowing us to estimate the antiplasticization temperature, $T_{anti} \approx 260$ K. At this temperature, the effect of the additive on the relaxation time evidently becomes inverted. We also observe that the curves rotate in a *clockwise* direction, indicating that the Aroclor causes PC to become plasticized at low temperatures (as evident in Figure 1), while it is predicted to become *antiplasticized* at higher temperatures (but still comparable to T_g). (Unfortunately, our current experimental setup can not access the frequency range required to directly observe this plasticization−antiplasticization transition in PC/Aroclor.) However, we have observed the full antiplasticization−plasticization transition in glycerol−trehalose mixtures.[5] In this case (inset in Figure 4), the rotation direction of the Arrhenius curves is *inverted* from the present observation on Aroclor−PC mixtures. The other inset in Figure 4 shows the T dependence of θ for Aroclor-PC mixtures, providing a different perspective on the same phenomenon, and this representation was also considered in our trehalose−glycerol study.[5] The crossing pattern of Arrhenius curves shown in Figure 4 has been reported before for the conductivity of both inorganic and organic semiconducting materials with impurities.[41] In this context, this crossing relation is referred to as the Meyer−Neldel rule.[41]

IV. A Simple Model of Additive-Induced Changes in High-Frequency Dynamics

A. Formal Application of Transition State Theory to the Dynamics of Mixtures. High-frequency relaxation processes characteristically exhibit an Arrhenius temperature dependence, so we may profitably adopt the Eyring transition state theory[3,4] framework to estimate θ. In particular, we may formally write θ within transition state theory[3,4] as

$$\theta = \exp(\delta G^+_{(\text{mixture})}/RT) \tag{6}$$

where $\delta G^+ = G^+_{(\text{mixture})} - G^+_{(\text{pure})}$ and $G^+_{(\text{mixture})}$ and $G^+_{(\text{pure})}$ are activation free energies of the high-frequency relaxation process under investigation in the fluid mixture and in the pure liquids, respectively. The activation free energy is then,

$$G^+ = E^+ - TS^+ \tag{7}$$

where E^+ and S^+ are the enthalpies and entropies of activation so that the change in the activation energy[4] upon dilution $\delta G^+_{(\text{mixture})}$ can be decomposed into enthalpic contributions:

$$\delta G^+_{(\text{mixture})} = \delta E^+_{(\text{mixture})} - T\delta S^+_{(\text{mixture})} \tag{8}$$

Transition state theory implies that θ is defined as

$$\theta = \frac{\tau_{(\text{mixture})}}{\tau_{(\text{pure})}} = \frac{\tau_{\infty(\text{mixture})} \exp(E^+/RT)}{\tau_{\infty(\text{pure})} \exp(E^+/RT)} \tag{9}$$

where $E^+_{(\text{mixture})} \equiv E^+_m$ and $E^+_{(\text{pure})} \equiv E^+_0$ are the observed activation energies of the mixture and the pure solvent, respectively, and $\tau_{\infty(\text{mixture})} \equiv \tau_{\infty m}$ and $\tau_{\infty(\text{pure})} \equiv \tau_{\infty 0}$ are the corresponding relaxation time prefactors. We then identify δE^+_m and δS^+_m as

$$\delta E^+_m = E^+_m - E^+_o \tag{10}$$

$$\exp(-\delta S^+_m/R) = \tau_{\infty m}/\tau_{\infty 0} \tag{11}$$

The problem of determining the change in the high-frequency relaxation time τ_β (more generally, the reaction rate in a chemical reaction context) then devolves to a consideration of the separate concentration dependences of δE^+_m and δS^+_m.

It is natural to assume, within this mean field theoretical description of the fluid dynamics, that the molecular species are homogeneously mixed and that δE^+_m and δS^+_m are analytic functions of concentration. We then formally expand δE^+_m and δS^+_m in a Taylor series in the concentration x_w of the diluting species,

$$E^+ = E^+_0 + (\mathrm{d}E^+_m(x_{w=0})/\mathrm{d}x_w)x_w + O(x_w{}^2) \tag{12}$$

$$S^+_m = S^+_0 + (\mathrm{d}S^+_m(x_{w=0})/\mathrm{d}x_w)x_w + O(x_w{}^2) \tag{13}$$

where O denotes the order of magnitude. When the concentration of the diluting species is small, which is often a *defining feature* of "diluent", a truncation of these series should be adequate, leading to the approximate relations

$$\delta E^+_m \approx (\mathrm{d}E^+_{m(c=0)}/\mathrm{d}c)x_w, \qquad \delta S^+_m \approx (\mathrm{d}S^+_{m(c=0)}/\mathrm{d}c)x_w \tag{14}$$

Similar formal arguments were made by Eyring and coworkers[42] in the context of estimating the viscosities of fluid mixtures, who also suggested that the linear concentration terms in eq 14 depends on the free-energy of mixing of liquids (and thus the osmotic virial coefficient), as well as the activation energies of the pure components. We take the views that δE^+_m and δS^+_m (or rather the change and the apparent activation energy and the prefactor of the Arrhenius relation; see eq 9) are measurable quantities that characterize the differential effect on the high-frequency dynamics of one fluid through the addition of another and, as such, provide a fundamental *metric* for how much the addition of one fluid alters the dynamics of the other. These parameters play a role similar to the second virial coefficient in describing thermodynamic interparticle correlation effects in gases and liquid mixtures, and thus their determination is fundamental to the construction of a theory of how dilution alters fluid dynamics.

Before proceeding, it should be noted that transition state theory is a highly idealized model of the dynamics of condensed fluids so that E^+ and S^+ should not be literally interpreted as enthalpies and entropies of activation of some local binary reaction process between molecules. In reality, the condensed state, especially the liquid state of complex fluids such as polymers at low temperatures, is characterized by *heterogeneity*,[29,43] and the measured relaxation rates reflect an averaging over this local structure. Molecular relaxation processes, even relatively

high-frequency processes, intrinsically involve cooperative molecular motion, as well as structural heterogeneity. Experimental studies of high-frequency ("β") relaxation processes in polymers have established that the apparent activation energy E^+ for such high-frequency processes depend strongly on chain molecular mass, but that these changes in E^+ saturate for a modest number of backbone atoms, and this phenomenon has reasonably been interpreted in terms of the local motion of groups of atoms defining the statistical segments of the polymer chains.[38] While the recognition of the existence of coarse-grained dynamical units within the polymer allows for a rationalization of the observed E^+, on the basis of extensions of original arguments relating E^+ to the intermolecular cohesive energy,[42] it is difficult to estimate the prefactor associated with these high-frequency molecular relaxation processes. This prefactor is coupled with entropic changes that occur through the hierarchical molecular rearrangement events involved in molecular displacements in the condensed state.

Experimentally, one can obtain the activation energy, E^+, and the pre-exponential factor τ_∞ from the Arrhenius temperature dependence of relaxation times (see eq 4). As we defined in our previous paper,[5] the pre-exponential factor of mixture and of the pure liquid are described by the relation

$$\tau_{\infty m}/\tau_{\infty 0} = \exp(\delta S^+_m/x_w R) \approx \exp([S^+_m]x_w) \quad (15)$$

$$[S^+_m] \equiv \lim_{x_w \to 0}(\delta S^+_m/x_w R) = (dS^+_{m(x_w=0)}/dx_w)/R \quad (16)$$

Equations 8 and 13 imply that θ should have a general exponential concentration dependence at low-to-moderate concentrations of additive,

$$\theta = \exp(Ax_w) \quad (17)$$

where A is correspondingly defined as

$$A = (\delta E^+_m/x_w RT) - (\delta S^+_m/x_w R) \approx ([E^+_m]/T) - [S^+_m] \quad (18)$$

$$[E^+_m] = \lim_{x_w \to 0}(\delta E^+_m/Rx_w) = (dE^+_{m(x_w=0)}/dx_w) \quad (19)$$

The parameters $[S^+_m]$ and $[E^+_m]$ are "virial coefficients" for the entropy and enthalpy of activation. In our previous work,[5] we denoted $[S^+_m]$ by $-[\tau_\infty]$, where the sign convention is notably *opposite* that of the current definition.

A dependence of θ on concentration consistent with eq 17 has been observed for numerous condensed phase systems, and some representative examples are indicated in Figure 5 to give some appreciation of the generality of the effect (see also Section IV.B). These examples include solvent reorientational relaxation in polymer solutions, dielectric relaxation in a sugar−alcohol mixture, and the rate of a classical chemical reaction in a solvent mixture. The figure panels are described as follows: (a) Schematic dependence of θ on concentration in mixtures exhibiting a plasticization−antiplasticization transition as a function of temperature. The figure illustrates the common physical situation, where antiplasticization occurs upon cooling and where the slope in this type of plot progressively decreases as the temperature is decreased. (b) Mean solvent reorientation time τ_s for Aroclor 1248 (polychlorinated biphenyl mixture with 48% chlorine) in polymer solutions normalized by its value in a neat solvent τ^0_s, versus polymer concentration in grams per mole × 100. Four different polymers are shown at two temperatures: polystyrene, polyisoprene, poly(1,2-butadiene), and poly(1,4-butadiene).[44] (c) Dielectric relaxation time data for trehalose diluted by glycerol at five different temperatures.[5] The data indicate the ratio of relaxation time of a secondary dielectric relaxation process of a trehalose−glycerol mixture relative to its value for pure trehalose. (d) The dependence of the rate constant of the Diels−Alder reaction of methyl vinyl ketone with cyclopentadiene in aqueous solutions on the addition of organic cosolvents.[45,46] This figure shows the Diels−Alder rate constant of the mixture k_m with the organic cosolvent relative to the pure aqueous solution k_0 (see also refs 47 and 48).

It is evident that the signs of $[E^+_m]$ and $[S^+_m]$ in eq 18 determine whether antiplasticization ($\theta > 1$) or plasticization ($\theta < 1$) is observed and whether a *transition* between these behaviors should occur as the temperature is varied from high to low T. In particular, if $[E^+_m]$ and $[S^+_m]$ have opposite signs, then no transition from plasticization to antiplasticization occurs, while, if the quantities have the same signs, then there is a compensation temperature T_{anti}[5] defined by $A = 0$ and $\theta = 1$ in eqs 17 and 18. This allows us to estimate the "antiplasticization temperature" T_{anti} explicitly as

$$T_{anti} = (dE^+_{m(c=0)}/dx_w)/(dS^+_{m(c=0)}/dx_w) \quad (20)$$

As noted in our previous work, the transition from antiplasticization to plasticization can occur under two distinct conditions corresponding to where ($[E^+_m]$, $[S^+_m]$) obey the sign relations (+, +) or (−,−). Physically, these mathematical conditions correspond to whether antiplasticization is observed at low temperatures (as usually the case) or whether it is observed at high temperatures. These qualitatively different patterns in the change of the rate of relaxation (or reaction kinetics) with diluent are readily recognized graphically, and the change in the rate of molecular relaxation rates with dilution can be classified into 10 different classes of behavior, of which the four relevant cases are schematically illustrated in Figure 6. Equations 16 and 17 imply that the Arrhenius curves for $\log(\tau)$ versus $1/T$ should rotate counter-clockwise about a fixed point (the antiplasticization temperature, T_{anti}) when the plasticization-to-antiplasticization transition occurs upon cooling (case I in Figure 6). In the opposite case, the predicted plasticization effect should occur upon cooling, and this rotation should occur in the *clockwise* direction (case II; see data presented in the following sections). In the next two cases, although the lines rotate, T_{anti} formally occurs for a negative temperature (cases III (counter-clockwise) and IV (clockwise rotation); not presented in the figure for simplicity) so that compensation does not occur for a finite T. There are also cases where no antiplasticization−plasticization compensation effect exists. When $[S^+_m]$ (or the entropy of activation) changes while $[E^+_m]$ remains constant, the Arrhenius curves for τ become translated either down or up, corresponding to a uniform decrease or increase of τ, respectively (cases V and VI; see ref 49). Correspondingly, when $[S^+_m]$ is constant and $[E^+_m]$ changes, only the slope of the curves changes, and no transition occurs (cases VII and VIII). Finally, there are cases where both $[S^+_m]$ and $[E^+_m]$ change and are proportional, but where these quantities have the opposite sign so that there is no condition where compensation can occur (cases IX and X). This situation has been termed "anti-compensation".[50]

B. Plasticization−Antiplasticization Transition and Entropy−Enthalpy Compensation. Since our previous work on trehalose−glycerol mixtures, we have realized that our observation of a plasticization−antiplasticization transition with temperature is actually a special case of a more general phenomenon termed "entropy−enthalpy compensation".[51] The compensation condition $\theta = 1$ indeed means that the enthalpy and entropies of activation change by dilution *compensate* each other. Our analysis indicates that, while this phenomenon may be common,

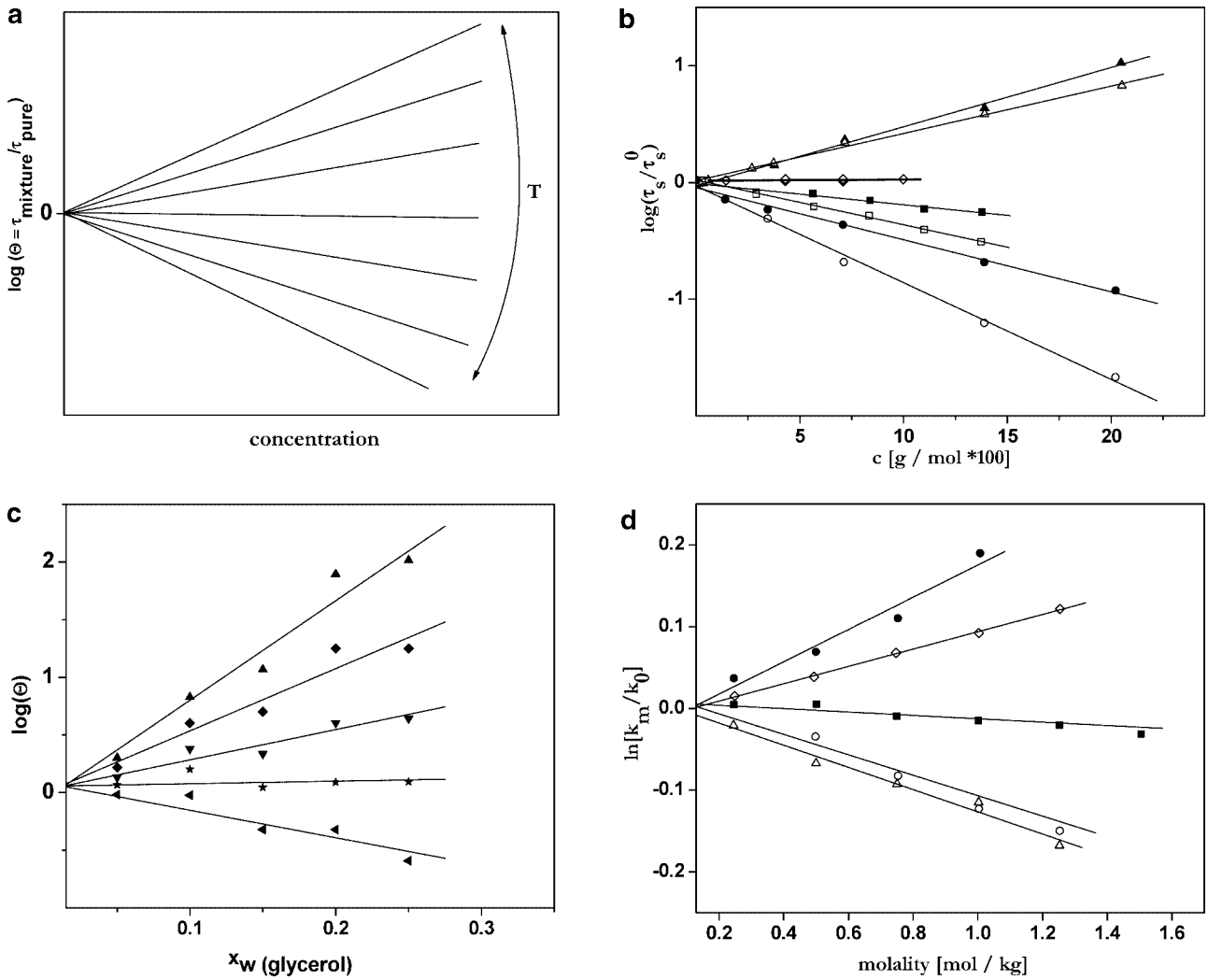

Figure 5. (a) Concentration dependence of $\theta = \tau_{(\text{mixture})}/\tau_{(\text{pure})}$ under various temperature conditions. Schematic concentration dependence of θ in a system exhibiting antiplasticization. There are two classes of antiplasticizers, corresponding respectively to an increase or decrease of the slope indicated with cooling (see text for explanation). (b) Solvent rotational relaxation time for Aroclor 1248 as a function of polymer concentration at various constant temperatures (figure reprinted with permission from ref 44). (c) Dielectric relaxation time of trehalose diluted by glycerol at various temperatures; concentrations given in glycerol weight fraction.[5] (d) Kinetics of reactions in aqueous solutions of organic fluids (figure reprinted with permission from ref 45).

it is not universal. For example, the catalytic behavior of some proteins and catalysts revolve around their acting to shift θ to uniformly larger values,[49] corresponding to case V of Figure 6.

We examine this entropy−enthalpy compensation phenomenon in some detail for our diluted PC measurements in Figure 7. The insets show the Aroclor concentration dependence of the apparent activation energy E^+ and $\log(\tau_\infty)$. The figures reveal that the concentration dependence of E_m^+ and S_m^+ is linear at least in the investigated range of concentrations. In Figure 7, we also observe that $\log(\tau_\infty) \propto S_m^+$ varies in near proportionality to E_m^+. This is a classic entropy−enthalpy compensation plot,[51] and Table 1 enumerates some other particular systems where this effect has been observed. We see that this ("repeatedly discovered") phenomenon is found rather frequently in both the chemical reaction kinetics and the relaxation dynamics of condensed phases (both liquids and solids), and this phenomenon even arises in heterogeneous gas phase catalysis. Liu and Guo[51] provide an extensive review of entropy−enthalpy compensation, including many further examples and discussion of the issues these observations raise. Entropy−enthalpy compensation is evidently at the heart of the plasticization−antiplasticization transition.

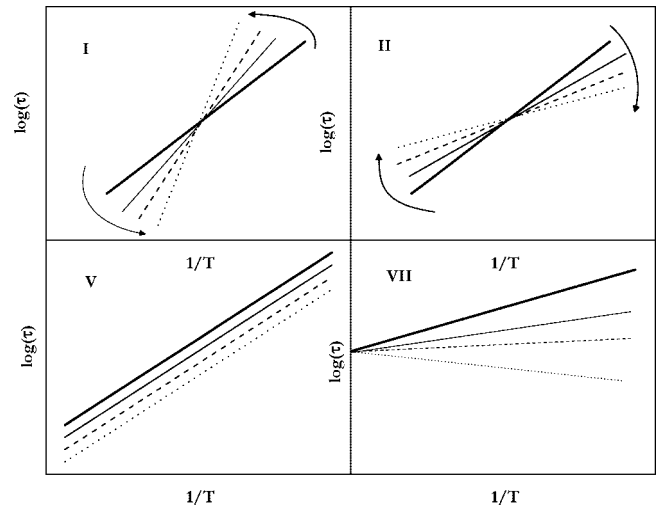

Figure 6. Schematic indication of different classes of plasticization−antiplasticization. Thick solid lines represent pure systems, and the other lines indicate curves obtained progressively increasing the concentration of the additive (lowest concentration = solid line; intermediate concentration = dashed line; highest concentration = dotted line). See text for further description.

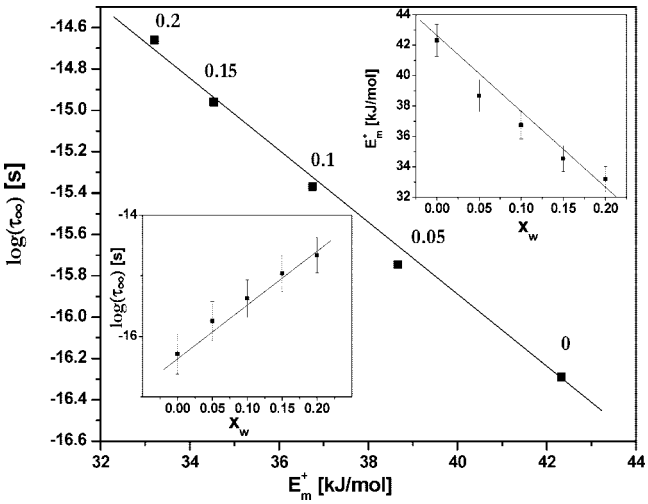

Figure 7. Prefactor from Arrhenius function versus activation energy for different PC−Aroclor mixtures. The insets present $\log(\tau_\infty)$ and E_m^+ for mixtures with corresponding Aroclor concentrations.

Although a full molecular understanding of entropy−enthaply compensation can be expected to involve subtle many-body effects, Dyre[52] and Vainas[53,54] have provided valuable qualitative insights into this difficult problem. For example, Dyre notes that, if the relaxation process involves an exponential distribution of barrier heights, reflecting the local structural heterogeneity of the disordered material, then atomic displacements becomes correspondingly intermittent. He then notes that this situation leads to a relaxation process in which the entropy and enthalpy of activation of structural relaxation exhibit compensating changes and to a corresponding power law relaxation associated with the intermittent molecular displacements. Our observation of HN relaxation and entropy−enthalpy compensation in our β dielectric relaxation measurements are *both* qualitatively consistent with Dyre's heuristic arguments. Vainas has also provided some insight into this ubiquitous phenomenon by exactly solving a model of relaxation on a hierarchical lattice (Cayley tree) in which the activation entropy is precisely tunable in terms of lattice geometry. Vainas' model exactly leads to entropy−enthalpy compensation. Moreover, Dyre has argued that the enthalply−entropy compensation temperature (T_{anti}) can be identified with the VF temperature, where local relaxation "freezes". This suggests an interesting possible direct connection between the entropy−enthaply compensation phenomenon and the physics of glass-formation for the high-frequency dynamics studied in the present work.

We emphasize that our recognition that the antiplasticization−plasticization transition in our dielectric relaxation measurements corresponds to enthalpy−entropy compensation within transition state theory does not really explain this phenomenon. Enthalpy−entropy compensation has been characterized as one of the most general, but least theoretically understood phenomenon of the physical chemistry of liquids.[51] While it certainly makes sense heuristically that a stronger enthalpic interaction in the transition state can reasonably be expected to lead to a reduced magnitude of the activation entropy because of the more constrained motions in the transition state,[55,56] it is difficult to translate this qualitative reasoning into any kind of precise theoretical predictions for T_{anti}.

V. Evidence for Plasticization−Antiplasticization Transition from Neutron Scattering and Mechanical Measurements

Antiplasticization by a diluent is also characterized by material stiffening, despite the contrary general trend of a reduction of T_g[6,57,58] with the addition of molecular additives. It should then be possible to observe this phenomenon in high-frequency dynamics measurements such as neutron or X-ray scattering through measurements of the Debye−Waller factor[20,60] or through direct mechanical properties measurements such as the storage modulus of the diluted polymeric material (G'). Notably, the rheological measurements normally involve a much lower frequency regime than the neutron and secondary relaxation dielectric measurements that include the α-relaxation processes associated with cooperative segmental motions, as well as much slower relaxation processes associated with large-scale chain motions so that comparisons to high-frequency dielectric measurements must be performed appropriately. Despite these different frequency ranges, a tendency toward stiffening with dilution can be expected in conjunction with antiplasticization in these measurements. We are concerned in this section with confirming that these changes are at least qualitatively consistent with the dielectric measurements, given the greatly different frequency ranges explored in these "high-frequency" measurements.

A. Neutron Scattering. In Figure 8, we illustrate the T dependence of the average mean squared hydrogen atom displacement $\langle u^2 \rangle$ in our PC material diluted by Aroclor. For our samples below T_g, but *above* the dielectric antiplasticization temperature $T_{anti} \approx 260$ K, we observe that the average slope describing the T dependence of $\langle u^2 \rangle$ becomes reduced with increasing Aroclor concentration. Within a simple harmonic localization model, this slope can be described as being inversely proportional to a molecular "force constant" κ,[20,60]

$$\langle u^2 \rangle \approx (k_B T)/\kappa \tag{21}$$

and we plot κ based on this simple approximation (made in the temperature range of 200−350 K) in the figure inset. We thus infer a progressive local *stiffening* of the polymeric material in the temperature range $T > T_{anti}$, despite the fact that the addition of Aroclor causes an appreciable drop in T_g. This trend is consistent with antiplasticization behavior and with the high-frequency dielectric relaxation time data shown in Figure 4. However, the neutron data does not reveal an overt transition to plasticization in the low temperature glass state, an effect clearly indicated by the dielectric data in Figure 1. (At very low temperatures, the neutron scattering data is noisy, and it is frankly difficult to resolve any clear trend.) We also note that the side-group (methyl group, in particular) rotations give a large contribution to $\langle u^2 \rangle$ so that simplistic interpretation of $\langle u^2 \rangle$ as a measure of local material "stiffness" must be made with due caution; neutron measurements by themselves provide an inconclusive measure of plasticization or antiplasticization. References 60−62 discuss issues that arise from methyl rotation effects that arise in relation to interpreting dynamic neutron scattering measurements.

B. Mechanical Measurements. An antiplasticization−plasticization effect of PC with the addition of Aroclor is an established effect in mechanical measurements,[63] giving us greater confidence in the qualitative validity of the antiplasticization effect suggested by the dynamic neutron measurements. Since there have been many previous studies of this phenomenon in this classical model system, we only briefly illustrate this effect here. In Figure 9, we show the storage modulus at a fixed

TABLE 1: Examples for Entropy−Enthalpy Compensation Reported in Literature

entropy−enthalpy compensation			
reactions in organic chemistry	refs 45−47, 69	influence of salt on viscosity of salt solutions	ref 70
enzyme catalysis	refs 71, 72	ionic conductivity of glasses	refs 73, 74
viscosity of simple and polymer liquids at high temperatures	refs 75−77	diffusion in crystalline solids	refs 78, 79
conductivity of organic substances	refs 41, 80	electrical conductivity of single crystals	ref 81
heterogenous catalysis	refs 82−84	oxygen binding in myoglobin and other proteins	ref 85
thermally induced virus inactivation	ref 86	pH effect on protein denaturation	ref 87
thermal death of bacteria and yeast	ref 88	thermal decomposition reactions of inorganic substances	ref 89
evolutionary adaptations of proteins	ref 90	protein unfolding	ref 91

frequency ($f = 1$ Hz) as a function of temperature for our pure and diluted PC samples. The figure shows that the addition of Aroclor to PC leads to a softening (plasticization) of the material well below the antiplasticization temperature T_{anti}, which was determined from the dielectric measurements (vertical dotted line), and a stiffening (antiplasticization) of the material at higher temperatures than T_{anti}. This trend reverses again for temperature well above T_g, where plasticization is again observed, reflecting the downward shift of T_g with Aroclor addition. Although the inversion temperature between plasticization and antiplasticization in the mechanical measurements is not very sharply defined, the qualitative trend observed in these measurements is quite consistent with changes in the dynamics indicated by the dielectric and neutron scattering measurements. We note that the relatively low and fixed frequency of these mechanical measurements makes the apparent antiplasticization temperature occur at an appreciably lower temperature (≈ 40 K lower) than the antiplasticization temperature estimated in the β dielectric relaxation measurements (see Figure 4). Nonetheless, an overall stiffening of the mixture in the glassy state well below T_g can be observed as a result of the antiplasticization of the high-frequency relaxation dynamics of the polymer material through the addition of Aroclor, while at higher temperatures, plasticization is found. Similar observations have been made before for PC diluted by different Aroclors having a range of molecular masses (5460, 1254, 1232),[63] where the molecular mass is found to influence quantitative aspects of the antiplasticization effect, such as the particular value of T_{anti}.

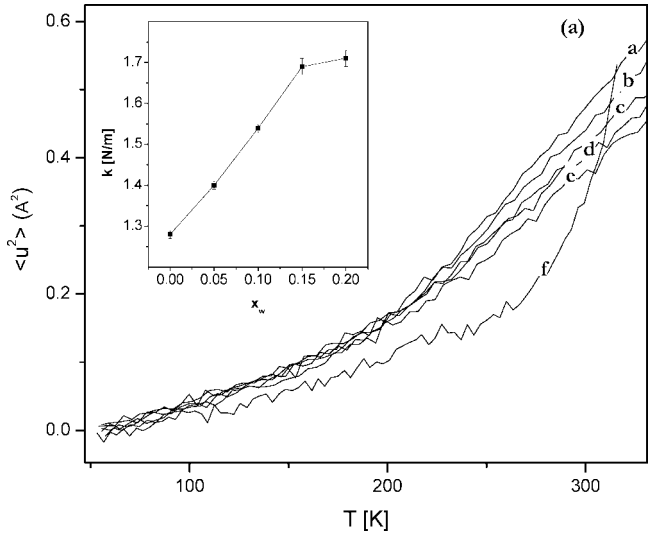

Figure 8. Quasi-elastic neuron scattering data as a function of temperature: pure PC (a), mixtures with Aroclor mass fraction, x_w: 0.05 (b), 0.1 (c), 0.15 (d), and 0.2 (e), and pure Aroclor (f). Inset presents the effective force constant k as a function of Aroclor concentration; the values are obtained from fitting for $T = 200-350$ K.

VI. Conclusions

We further develop a theoretical framework for characterizing how the high frequency of fluids becomes modified upon the addition of fluid and nanoparticle additives. The framework indicates that there are eight distinct patterns of behavior that should occur. Two of these patterns involve the cases where antiplasticization (slowing down of the system dynamics) or plasticization (speeding up of these dynamics) always occurs regardless of the temperature. The other two cases correspond to the cases where a transition from plasticization to antiplasticization occurs upon varying T. While the case of a transition from plasticization to antiplasticization upon cooling appears to be the more common situation experimentally in diluted polymer melts, we observe the opposite case in our measurements on PC diluted by Aroclor. We also find that the fragility of glass-formation progressively increases with the addition of Aroclor, a trend opposite to our previous experience with mixtures of trehalose diluted by glycerol.[5] Apart from the main applications of antiplasticization to materials processing enhanced abrasion resistance of films in photographic and laser printer films[64] and food and drug preservation,[6,59,65] our approach to quantifying the changes in the high frequency of diluted fluids should provide a powerful metric for understanding and controlling property changes related to dynamics and reaction processes in a wide range of mixtures, including the important case of aqueous solutions where alcohols, polymers, and salts additives can have an appreciable effect on the dynamics without any clear thermodynamic explanation. The combination of our theoretical framework with dielectric spectroscopy or other methods that allow for probing the high frequency in a routine

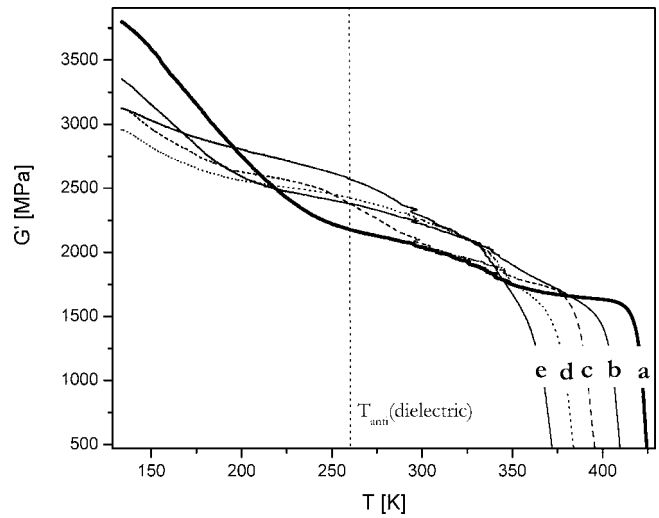

Figure 9. Storage modulus from DMA measurements: pure PC (a), mixtures with Aroclor mass fraction, x_w: 0.05 (b), 0.1 (c), 0.15 (d), and 0.2 (e).

fashion, should allow for the characterization of many complex fluid mixtures in connection with their applications exploiting or relying on control of changes in the dynamics that accompany the dilution process.

Complex fluids, such as polymer melts, are often characterized by high-frequency molecular relaxation processes that can be identified by a variety of experimental methods. Future work should consider the extent to which the changes in the high frequency dynamics depend on the relaxation process examined. It is evidently important that the changes in the high frequency dynamics determined by our method correspond to property changes of interest in the diluent modified material (e.g., gas permeability[23,66] and stiffness[23,64]) so that the high-frequency measurements inform about these property measurements, as well as other high-frequency domain measurements. This question requires further consideration.

In future work, we also plan to investigate whether the inverted trends in fragility changes with additive, seen in adding glycerol to trehalose and Aroclor to PC, are related to the corresponding inversion in the antiplasticization−plasticization transitions with temperature. Simulation has recently indicated,[24−27] in accord with the entropy theory of glass-formation developed by Dudowicz et al.,[38,67] that reducing packing frustration tends to reduce the fragility of glass-formation, so that the increase of fragility upon the addition of an additive can naturally be understood by an increase of the fragility of glass-formation. The addition of fullerene particles to polystyrene polymer matrix has indicated an appreciable increase in the Debye−Waller factor in the low temperature glass state,[68] pointing to an *increased* fragility of the nanocomposite, an effect that we expect is quite common. In the near future, we plan to check the attractive possibility that additives that enhance or disrupt the molecular packing of the pure fluid correspondingly lead to antiplastization and plasticization, respectively, in the glass state well below T_g. If this proves to be true, then it would provide a valuable design tool for the properties of diverse mixtures.

Acknowledgment. K.A.P. gratefully acknowledges support from the National Research Council Associateship program. This work utilized facilities supported in part by the National Science Foundation under Agreement No. DMR-0454672. The authors are also grateful to C. M. Roland in the Naval Research Laboratory for the supply of Aroclor sample and to Jong Keun Park and Robert B. Moore at The University of Southern Mississippi for their dynamic mechanical measurements. The materials and equipment identified in this paper are for descriptive purposes only and do not imply endorsement by the National Institute of Standards and Technology.

References and Notes

(1) Jackson, W. J., Jr; It, Caldwell *J. Appl. Polym. Sci.* **1967**, *11*, 216–226.

(2) Yee, A. F.; Smith, S. A. *Macromolecules* **1981**, *14*, 54.

(3) Hill, N. E.; Vaughhan, W. E.; Price, A. H.; Davis, M. *Dielectric Properties and Molecular Behavior*; Reinhold: London, 1969; pp 69−71.

(4) Gladstone, S.; Laidler, K. J.; Eyring, H. *The Theory of Rate Processes*; McGraw-Hill: New York, 1941. The identification of the activation energy and the enthalpy of activation neglects the temperature dependence of the "transmission coefficient" prefactor in the Eyring "absolute rate theory" expression for the relaxation time since many physical factors contribute to this factor [Chandler, D. *J. Stat. Phys.* **1986**, *42*, 49] in the condensed state. Formally, the activation energy in eq 4 differs from the enthalpy of activation by an additive constant, RT, where R is the gas constant [Starkweather, H. W. *Macromolecules* **1981**, *14*, 1277].

(5) Anopchenko, A.; Psurek, T.; VanderHart, D.; Douglas, J. F.; Obrzut, J. *Phys. Rev. E* **2006**, *74*, 031501.

(6) Seow, S. C.; Cheah, P. B.; Chang, Y. P. *J. Food Sci.* **1999**, *64*, 576.

(7) Dirama, T. E.; Carri, G. A.; Sokolov, A. P. *J. Chem. Phys.* **2005**, *122*, 114505.

(8) Riggleman, R. A.; Yoshimoto, K.; Douglas, J. F.; de Pablo, J. J. Trehalose and glycerol. *J. Chem. Phys.*, in press.

(9) Johari, G. P.; Goldstein, M. *J. Chem. Phys.* **1970**, *53*, 2372.

(10) (a) Fujimori, H.; Oguni, M. *Solid State Commun.* **1995**, *94*, 157 See also (b) Bershtein, V. A.; Egorov, V. M; Emelyanov, I. A; Stepanov, V. A *Polym. Bull.* **1983**, *9*, 98.

(11) Frick, B. *Prog. Colloid Polym. Sci.* **1989**, *80*, 164.

(12) Frick, B.; Fetters, L. J. *Macromolecules* **1997**, *27*, 974.

(13) Frick, B; Richter, D. *Science* **1995**, *267*, 1939.

(14) Colmenero, J.; Arbe, A. *Phys. Rev. B* **1998**, *57*, 13508.

(15) Angell, C. A.; Ngai, K. L.; McKenna, G. B.; McMillan, P. F.; Martin, S. W. *J. Appl. Phys.* **2000**, *88*, 3113.

(16) Doster, W.; Cusack, S.; Petry, W. *Nature* **1989**, *337*, 754.

(17) Angell, C. A. *Science* **1995**, *267*, 1924.

(18) Lehnert, U.; Réat, V.; Weik, M.; Zaccaï, G.; Pfiester, C. *Biophys. J.* **1998**, *75*, 1945.

(19) Deriu, A. *Neutron News* **2000**, *11*, 26.

(20) Zaccaï, G. *Science* **2000**, *288*, 1604.

(21) Cauley, B. J.; Cipriani, C.; Ellis, K.; Roy, A. K.; Jones, A. A.; Ingiefield, P. T.; McKinley, B. J.; Kambour, R. P. *Macromolecules* **1991**, *24*, 403.

(22) (a) Rizos, A. K.; Petihakis, L.; Ngai, K. L.; Wu, J.; Yee, A. *Macromolecules* **1999**, *32*, 7921. (b) Xiao, C.; Wu, J.; Yang, L.; Yee, A. F.; Xie, L.; Gidley, D.; Ngai, K. L.; Rizos, A. K. *Macromolecules* **1999**, *32*, 7913.

(23) Maeda, Y.; Paul, D. R. *J. Polym. Sci. B, Polym. Phys.* **1987**, *25*, 957.

(24) Riggleman, R. A.; Yoshimoto, K.; Douglas, J. F.; de Pablo, J. J. *Phys. Rev. Lett.* **2006**, *67*, 405502.

(25) Riggleman, R. A.; Douglas, J. F.; de Pablo, J. J. *J. Chem. Phys.* **2007**, *126*, 234903.

(26) Riggleman, R. A.; Douglas, J. F.; de Pablo, J. J. *Phys. Rev. E* **2007**, *76*, 011504.

(27) Abraham, S. E.; Bhattacharrya, S. M.; Bagchi, B. *Phys. Rev. Lett.* **2008**, *100*, 167801.

(28) Havriliak, S.; Negami, S. J. *J. Polym. Sci., Part C* **1996**, *14*, 99.

(29) Douglas, J. F.; Hubbard, J. B. *Macromolecules* **1991**, *24*, 3163.

(30) Douglas, J. F. *J. Phys.: Condens. Matter* **1999**, *11*, A329.

(31) Cole, K. S.; Cole, R. H. *J. Chem. Phys.* **1941**, *9*, 341.

(32) Kremer, F.; Schonhals, A. *Broadband Dielectric Spectroscopy*; Springer: Berlin, 2003.

(33) Ngai, K. L.; Capaccioli, S. *Phys. Rev. E* **2004**, *69*, 031501.

(34) Adams, J. A.; Gibbs, E. A. *J. Chem. Phys.* **1965**, *43*, 139.

(35) Hodge, I. M. *J. Non-Cryst. Solids* **1994**, *169*, 211.

(36) (a) Vogel, H. *Phys. Z.* **1921**, *22*, 645. (b) Fulcher, G. S. *J. Am. Ceram. Soc.* **1923**, *8*, 789.

(37) Martinez, L.-M.; Angell, C. A. *Nature* **2001**, *410*, 663.

(38) Dudowicz, J.; Douglas, J. F.; Freed, K. F. *Adv. Chem. Phys.* **2008**, *137*, 125.

(39) Branca, C.; Magazù, S.; Maisano, G.; Migliardo, P.; Villari, V.; Sokolov, A. P. *J. Phys.: Condens. Matter* **1999**, *11*, 3823.

(40) Chen, B.; Sigmund, E. E.; Halperin, W. P. *Phys. Rev. Lett.* **2006**, *96*, 145502.

(41) Rosenberg, B.; Bhowmik, B. B.; Harder, H. C.; Postow, E. *J. Chem. Phys.* **1968**, *49*, 4108.

(42) Kinkaid, J. F.; Eyring, H.; Stearn, A. E. *Chem. Rev.* **1941**, *28*, 301.

(43) Douglas, J.; Dudowicz, J.; Feed, K. F. *J. Chem. Phys.* **2006**, *125*, 144907. For earlier discussions of dynamic heterogeneity in this work, see refs 13, 14, 26, and 27 of this work.

(44) Lodge, T. P. *J. Phys. Chem.* **1993**, *97*, 1480.

(45) Blokzijl, W.; Blandamer, M. J.; Engberts, J. B. F. N. *J. Am. Chem. Soc.* **1991**, *113*, 4241.

(46) Blokzijl, W. Organic reactivity in mixed aqueous solvents: A link between kinetics and thermodynamics. Ph.D. Thesis, Univ. of Groningen, 1991.

(47) Giese, B. *Acc. Chem. Res.* **1984**, *17*, 438.

(48) Eckert, C. A.; Hsieh, C. K.; McCabe, J. R. *AIChE J.* **1974**, *20*, 20.

(49) Sievers, A.; Beringer, M.; Rodnina, M. V.; Wolfenden, R. *Proc. Natl. Acad. Sci. U.S.A.* **2004**, *101*, 7897.

(50) Exner, O. *Prog. Phys. Org. Chem.* **1973**, *10*, 411.

(51) Liu, L.; Guo, Q.-X. *Chem. Rev.* **2001**, *101*, 673.

(52) Dyre, J. C. *J. Phys. C* **1986**, *19*, 5655.

(53) Veinas, B. *J. Phys. C* **1986**, *21*, L-341.

(54) Veinas, B. *J. Phys.: Condens. Matter* **1991**, *3*, 3941.

(55) Williams, D.; Searle, M.; Mackay, J.; Gerhard, U.; Maplestone, R. *Proc. Natl. Acad. Sci. U.S.A.* **1993**, *90*, 1172.

(56) Krishnamurthy, V. M.; Bohall, B. R.; Semetey, V.; Whitesides, G. M. *J. Am. Chem. Soc.* **2006**, *128*, 5802.

(57) Jackson, W. J., Jr.; Caldwell, J. R *Adv. Chem. Ser.* **1965**, *48*, 185.

(58) Bergquist, P.; Zhou, Y.; Jones, A. A.; Inglefield, P. T. *Macromolecules* **1999**, *32*, 7925.
(59) Cicerone, M. T.; Soles, C. L. *Biophys. J.* **2004**, *86*, 3836.
(60) Soles, C. L.; Dimeo, R. M.; Neumann, D. A.; Kisliuk, A.; Sokolov, A. P.; Liu, J.; Yee, A. F.; Wu, W. *Macromolecules* **2001**, *34*, 4082.
(61) Saviot, L.; Duval, E.; Jal, J. F.; Dianoux, A. J. *Eur. Phys. J.* **2000**, *17*, 661.
(62) Soles, C. L.; Douglas, J. F; Lin, E. K.; Lenhart, J. L.; Jones, R. L.; Wu, W. *J. Appl. Phys.* **2003**, *93*, 1978.
(63) Petrie, S. E. B.; Moore, R. S.; Flick, J. R. *J. Appl. Phys.* **1972**, *43*, 4318.
(64) Cais, R. E.; Nozomi, M.; Kawai, M.; Miyake, A. *Macromolecules* **2001**, *25*, 4588.
(65) Jagannath, J. H.; Jayaraman, K. S.; Arya, S. S. *J. Appl. Poym. Sci.* **1999**, *71*, 1147.
(66) Zhang, P.; Whistler, R. L. *J. Appl. Polym. Sci.* **2004**, *93*, 2896.
(67) Douglas, J. F.; Dudowicz, J.; Feed, K. F. *J. Phys. Chem.* **2005**, *109*, 21350.
(68) Sanz, A.; Ruppel, M.; Douglas, J. F.; Cabral, J. T. *J. Phys.: Condens. Matter* **2008**, *20*, 104209.
(69) Bruice, T. C.; Benkovic, S. J. *J. Am. Chem. Soc.* **1964**, *86*, 418.
(70) Feakins, D.; Waghorne, W. E.; Lawrence, K. G. *J. Chem. Soc., Faraday Trans. 1* **1986**, *82*, 563.
(71) Wolfenden, R.; Snider, M.; Ridgway, C.; Miller, B. *J. Am. Chem. Soc.* **1999**, *121*, 7419.
(72) Williams, D. H.; Stephens, E.; O'Brien, D. P.; Zhou, M. *Angew. Chem., Int. Ed.* **2004**, *43*, 6596.
(73) Almond, D. P. *Mater. Chem. Phys.* **1989**, *23*, 211.
(74) Almond, D. P.; West, A. R. *Solid State Ionics* **1987**, *23*, 27.
(75) van Krevelen, D. W.; Hoftyzer, P. J. *Die Angew. Makromol. Chem.* **1976**, *52*, 101.
(76) Barer, R. M. *Trans. Farad. Soc.* **1943**, *39*, 48.
(77) Waring, C. E.; Becher, P. *J. Chem. Phys.* **1947**, *15*, 488.
(78) Dosdale, T.; Brook, R. J. *Solid State Ionics* **1983**, *8*, 297.
(79) Dienes, G. J. *J. Appl. Phys.* **1950**, *21*, 1189.
(80) Kemeny, G.; Rosenberg, B. *J. Chem. Phys.* **1970**, *52*, 4151.
(81) Weichman, F. L.; Ku, R. *Can. J. Phys.* **1970**, *48*, 63.
(82) Taylor, J. L.; Ibbotson, D. E.; Weinberg, W. H. *J. Chem. Phys.* **1978**, *69*, 4298.
(83) Kang, H. C.; Jachimowski, T. A.; Weinberg, W. H. *J. Chem. Phys.* **1990**, *93*, 1418.
(84) Constable, F. H. *Proc. R. Soc. London, Ser. A* **1925**, *108*, 355.
(85) Wang, M.-Y. R.; Hoffman, B. M.; Shire, S. J.; Gurd, F. R. N. *J. Am. Chem. Soc.* **1979**, *101*, 7394.
(86) Barnes, R.; Vogel, H.; Gordon, I. *Proc. Natl. Acad. Sci. U.S.A.* **1969**, *62*, 263.
(87) Sukhorov, B. I.; Likhtenstein, G. I. *Biofizyka* **1965**, *10*, 935.
(88) Rosenberg, B.; Kemeny, G.; Switzer, R. C.; Hamilton, T. C. *Nature* **1971**, *232*, 471.
(89) Zmijewski, T.; Pysiak, J. In *Proceedings of the 4th International Conference on Thermal Analysis*; Buzas, I., Ed.; Heyden: London, 1975; p 205.
(90) Johnson, I. A.; Goldspink, G. *Nature* **1975**, *257*, 620.
(91) Liu, L.; Yang, C.; Guo, Q.-X. *Biophys. Chem.* **2000**, *84*, 239.

JP8034314